

## **DATA GENERATION USING DIGITAL TWINS FOR THE DEVELOPMENT OF CONDITION MONITORING ALGORITHMS – APPLICATION ON ROLLING ELEMENT BEARINGS**

**SHUBHAM SHARMA<sup>\*</sup>, MARCEL WIEMANN<sup>\*</sup> AND PETER KRAEMER<sup>\*</sup>**

<sup>\*</sup> Chair of Mechanics with a focus on Structural Health Monitoring (MSHM)  
University of Siegen  
Campus Paul Bonatz, 57076 Siegen, Germany  
e-mail: [shubham.sharma@uni-siegen.de](mailto:shubham.sharma@uni-siegen.de), [www.uni-siegen.de/mb/shm](http://www.uni-siegen.de/mb/shm)

**Abstract.** Most condition monitoring (CM) algorithms today are developed solely based on measured data. Development exclusively based on empirical procedures may lead to potential disadvantages as the measurement data can be impacted by unknown factors such as environmental changes, measurement disturbances, load changes, and signal-to-noise ratios. This "pollution" of data negatively affects understanding the algorithm's "reaction" to various faults or changes in operational conditions. It can also be challenging to produce and measure many realistic fault characteristics experimentally. But understanding the effects of different faults and changing load conditions on faults indicators is crucial for evaluating the algorithm's performance and limitations or for creating databases for algorithms using supervised learning techniques. This paper focuses on enhancing fault detection through digital twins by creating a data generation tool to evaluate the effectiveness of various CM algorithms for detecting damage in rolling element bearings. A structured methodology was employed to create a digital twin of a laboratory rotary test stand used for ball-bearing fault analysis using COMSOL's Multibody simulation environment. The simulation software allows for integrating multiphysics phenomena into a single environment, providing a flexible tool that can impose various application-specific conditions on the monitored asset at specified operating conditions. The Twin is partitioned based on the physical asset into two distinct subassemblies, the motor and the bearing track. The modelling of contact and friction within the bearings was achieved using COMSOL's Penalty Contact method. The Twin's performance is assessed by comparing the vibration signals obtained from an accelerometer positioned on the physical machine with those obtained from a virtual acceleration probe located in the same position on the simulated asset. The simulated and the measured signals are both analysed using envelope analysis. The developed twin model generated harmonic vibrations at the rated fault frequencies, exhibiting a desirable similarity to the vibration spectrum of the actual system when considering outer-race and inner-race faults. The proposed tool provides the ability to simulate failures in complex conditions enabling the extraction of data from virtually any machine location, enhancing datasets used for fault classification and prediction and supporting the development of more sophisticated algorithms for CM.

**Key words:** Condition Monitoring; Digital Twin; Ball Bearing Fault Analysis; Penalty Method; Rigid Body Contact

## 1 INTRODUCTION

The emergence of Industry 4.0, big data, and predictive maintenance has heightened the demand for dependable condition indicators that enable early fault detection and optimal maintenance scheduling [1]. Health indicators used in CM are trained for classifying and trending future machine health [2]. The effectiveness of such systems is highly dependent on the availability of reliable machine condition data. However, increased reliance on fault data recording, under different failure scenarios and testing quality incur substantial physical and monetary costs and augmented modelling, maintenance time and effort. Obtaining on-site measurement data during fault conditions can be difficult and risky, potentially leading to equipment damage. Improper sensor placement can also reduce the accuracy of fault prediction, adding complexity to condition monitoring and detection. Digital Twin (DT) has been proposed to address these information-gathering gaps using artificial sensors. As an emerging method, DT models and simulates assets under various loads and environments to evaluate asset performance throughout their entire useful life cycle, exclusively in the digital realm [3] [4]. However, the definition of DT and its applications can vary considerably based on numerous factors, leading to an absence of a comprehensive framework for creating, implementing, and utilising these digital assets. The research conducted in this study addresses this problem and the need for additional fault data in a typical rotary machine by employing a model-based simulated version of an in-lab rotary drive train within a Multibody simulation environment in COMSOL. This approach considers and evaluates the vibrations of ball bearing alongside penalty-based contact mechanics of rigid bodies, using real machine vibration signals to assess the health of the rotary machine. By leveraging this methodology, the study aims to develop a more robust and reliable means of monitoring and maintaining intricate systems, contributing to the advancement and widespread adoption of DT technology.

## 2 DIGITAL TWINS

The fundamental concept of DTs can be traced back to a presentation by Dr Grieves in 2003, which aimed to conceptualise a product lifecycle management centre [3]. By leveraging the capabilities of DT, industries can optimise their operations and maintenance strategies, leading to enhanced efficiency and cost savings. The concept of Digital Twins can be interpreted in different ways depending on the context. It can be defined as an exact replica of a physical system or an array of sensors integrated to simulate the real-time condition of a model [5]. DTs are also used to encapsulate the Model-based systems engineering (MBSE) approach, which uses interdisciplinary methodologies to determine system properties [6]. MBSE-based DTs are different from CAD models or Internet of Things (IoT) devices because they describe system variables under various settings. The development of an MBSE-based DT involves physically modelling the system and its components, integrating kinematic and dynamic characteristics, fitting health parameters with virtual sensors, synchronising simulation and machine models by tuning key parameters, and performing simulations on the physics model using user input data. Finally, the simulation results are combined with measured machine component data to predict the asset's properties, leading to informed decisions and optimised maintenance strategies. Another emerging DT approach deals with

physics-based machine learning, which incorporates physics principles with machine learning algorithms to develop more accurate, reliable, and interpretable models [7].

Currently, a lot of research is being done in the field of simulation-based analysis of bearings. The general trend is to have the experimental data from analysis compared with the real sensor data obtained. Tyagi and Panigrahi [8] performed transient analysis of a bearing FEM model to detect incipient faults. They created a CAD model of a bearing with a minor crack on the outer race and conducted tests on a real system. Liu and Huang [2] proposed a method to generate faulty samples for training Machine learning models. FEM models with faults were used to obtain fault samples, and test sets were inserted into the trained ML model for fault classification. Misha and Samantaray [9] developed a Multibody model for deep groove ball-bearing fault analysis and compared simulated signals to measured signals from a lab test bench.

### 3 CONTACT FORCE MODEL

The contact mechanism of ball-bearing elements significantly influences the overall stiffness and vibrations induced by the bearing. The contact forces cause the balls rotation around the raceways. In this section, we discuss the consideration of contact constraints and friction in the proposed COMSOL Multibody Dynamics (MBD) model, specifically between all bearing balls, cages, and bearing raceways.

The Penalty-based method is widely used in contact problems and was originally introduced as an optimisation solution for equally constrained optimisation problems [10]. It explicitly eliminates unknown constraints and replaces them with penalisation when a constraint violation occurs. The penalty factor's increase is determined by the degree of constraint violation, and unlike the Lagrange multiplier, penalty methods do not require additional variables. The constraint condition is approximated using the penalty parameter, making contact an unconstrained optimisation formulation where only the displacement variable is unknown. While a simple contact simulation with relatively few points can work well, the penalty method is unreliable for complex geometries and many vertices unless small time steps are used [11]. Penalty methods were originally developed for applications subject to equality constraints, where the restraint  $d_N > 0$  (penalty force gap) is transformed into a function  $f(d_N)$  using Macaulay bracket functions (Figure 1). This approach weakly enforces contact constraints, allowing for some penetration of bodies due to the linear relationship between the contact force and gap. However, achieving the impenetrability condition, where the complete satisfaction of the contact condition is realised when the penalty parameter is infinite, can lead to poor numerical performance. Although the Macaulay bracket is simple to implement, it is computationally taxing and non-differentiable at the contact point, which can cause significant instabilities in the convergence of Newton solvers [12].

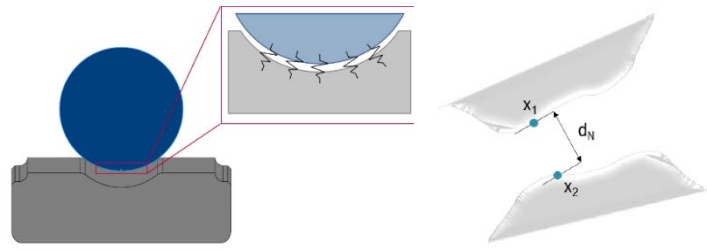


**Figure 1:** Penalty force in bearings (left), penalty gap (right)

### 3.1 MBD contact formulation

In MBD's rigid body contact node, there are two formulations of contact setting, the penalty and dynamic Penalty method [13]. The currently used build (COMSOL Multiphysics v5.6) of the Multibody Dynamics module only allows for rigid body contact [14]. The penalty method computes contact force based on the penalisation of the gap between the bodies such that there is no overlapping on either body by the other. It is formulated as equation 1:

$$\left( \begin{matrix} \cdot \\ \cdot \end{matrix} \right) \quad (1)$$

Here  $\cdot$  is the penalty factor, which depends on the diagonal distance of the bounding box of the geometries and the penalty factor multiplier. The penalty factor computes the stiffness of the spring in this contact, which prevents penetration of the rigid boundaries. The dynamic method also considers the viscous formulation for a transient simulation, as the contact forces depend on the rate of change in the gap. The dynamic force is given in equation 2 as:

$$\left( \begin{matrix} \cdot \\ \cdot \end{matrix} \right) \left( \begin{matrix} \cdot \\ \cdot \end{matrix} \left( - \right) \right) \quad (2)$$

The first part of the above computation considers the stiffness of the contact, and the second considers the damping or the viscous contact.  $\cdot$  is a time dependend viscous penalty factor. If the contact is only viscous controlled, then the viscous penalty factor also depends on further geometric properties of the contact bodies.

The distance between the contacting boundaries ( $\cdot$ ) is a fundamental quantity for rigid body contact (Figure 2). Interactions do not occur for positive gaps. For each node on the destination, the gap is calculated, and a corresponding node on the source boundary is found in the normal to the destination, this node as it approaches the destination, may not always be the closest available point. As the procedure converges, the gap reduces and approaches zero. Here, a centre-based contact method is used. The gap between the balls and the races is computed at every step. The gap is determined by the distance between the centres and the radii of the two bodies considered to be coming in contact. This parameter depends on the position of the two bodies in space. One of the bodies may be located inside the other, in that case the gap will depend on the inner boundaries of the two bodies. When the source is outside the destination (Equation 3):

$$(3)$$

and when the source is inside the destination (Equation 4):

(4)

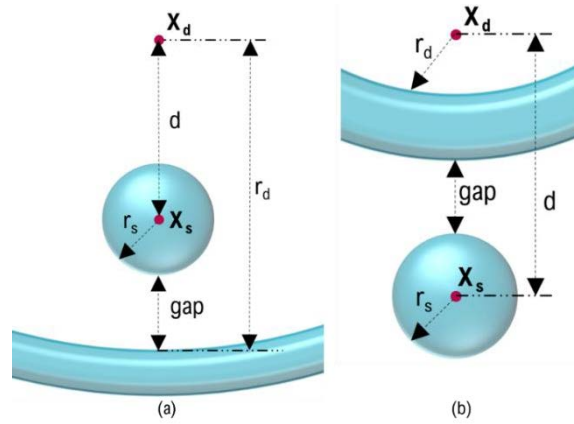


**Figure 2 :** Rigid body contact between ball and outer race, (a) source inside destination, (b) source outside destination

When friction is applied to bearing contacts, it can result from lubricated rolling motion and micro-slips between the surfaces of the ball and races, material inelasticity, and roughness. Although this contact is ideally a point contact, loads acting on the bearing cause the contact area to deform into an elliptical shape [15]. For this study, however, we assume point contact mechanics as the contacting bodies are non-elastic, and forces are computed at each contact point. The Coulomb friction model is used to model friction, allowing for a continuous friction law that can account for sliding and sticking as creeping between the contacting ball and raceways with a small relative velocity below the characteristic slip velocity [16]. The friction force in the rigid body contact node is given by equation 5:

$$\left( \begin{matrix} F_c \\ F_f \end{matrix} \right) \left( \begin{matrix} 1 \\ -1 \end{matrix} \right) \quad (5)$$

is the contact force, additional sliding resistance, the maximum friction force, is the slip velocity and is the characteristic slip velocity. distinguishes between the stick and slip friction contact conditions. Unless the static threshold is not achieved the contact pair is not permitted to move, i.e. stick mode. Once the threshold is crossed, the contact pair moves in the tangential direction, i.e. slip mode. The tangential force, combined with the contact forces, formulates the rotation of the balls around the races.

#### 4 METHODS

The experimental analysis of bearing faults utilised a rotary machine test station located at the SHM laboratory of the University of Siegen, as illustrated in Figure 3. The test station comprises two subassemblies, the motor track and the bearing track, which are firmly affixed

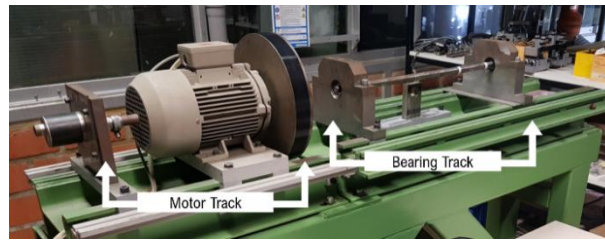


**Figure 3:** Bearing test station real model in University of Siegen MSHM lab

to the ground bench. The motor track has a Siemens three-phase AC motor (IEC90S), a flywheel, and a coupling connecting both subassemblies. The bearing track consists of three steel support pedestals for the three bearings (2x FAG 62303.2RSR and 1x SKF 61804). Artificial faults were introduced into bearings SKF 61804 bearings. To drive the motor, a Siemens VFD is utilised to provide three-phase power at a frequency of 50 Hz, and the motor speed is determined using a rotary encoder. The central bearing pedestal is designated for the test bearing, and the SKF 61804 bearings, induced with various faults, are mounted at this location. The acceleration of the central pedestal's top plate is measured using a PCB ICP accelerometer.

#### 4.1 Twin modelling

A combination of two COMSOL modules, namely the Multibody Dynamics (MBD) and the Rotating Machinery, Magnetic (RMM) interface, with interconnected constraints, is utilised to construct the Twin (Figure 4). The motor track and bearing track models only consider the essential geometric elements that multibody joints and constraints in COMSOL cannot replace. The design of the motor track is based on the stator and rotor forces considered in the analytical model developed by TEAM (Testing Electromagnetic Analysis Methods) [17]. The motor stator and rotor are defined in the Rotating Machinery, Magnetic (RMM) model as steel with an aluminium outer layer in the case of the rotor.

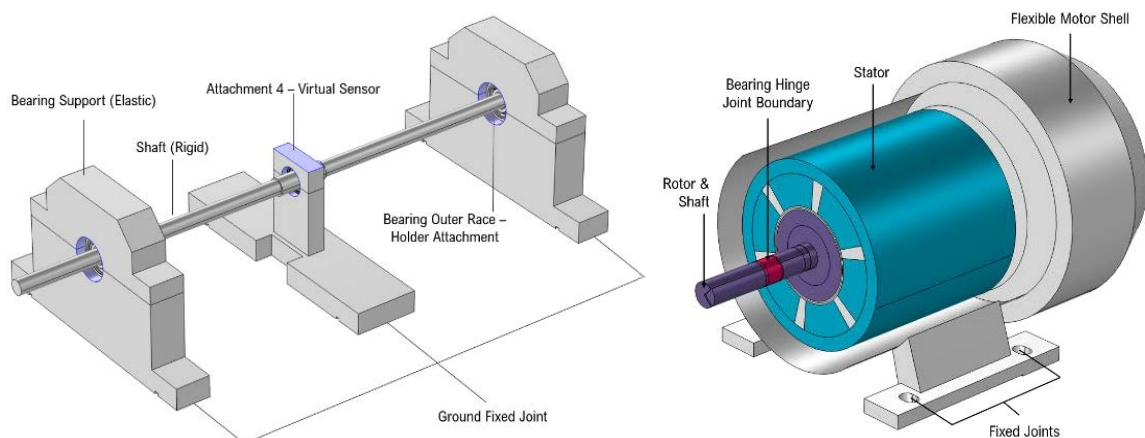


**Figure 4 :** Bearing Track Twin (left), Motor Track Twin (right)

The shaft and the bearings are considered rigid domains to associate MDB physics nodes,

while the other geometric features in MBD are deformable. The flywheel is replaced with a load boundary condition, which is applied on the primary shaft as force at the corresponding node. The shaft rotates at a fixed speed of 3000 rev/min, with the rotational torque and force variables from the RMM model in the case of the combined tracks or as a direct fixed rotation input via the prescribed displacement/rotation node in the case of the bearing track alone. The rotational speed is transmitted via rigidly fixed joints from the shaft to the inner races of the three bearings. The outer bearing races are fixed to the pedestal holder boundaries using flexible fixed joints to model significant structural stiffness and damping, keeping the bearings in position and restricting additional forces.

Simulated faults are introduced into the raceways of the twin model (SKF 61804, central bearing) to replicate the original defects present in the real system. Four faults are modeled. The first fault is a hole in the outerring (Figure 5 a). The second fault is a in the innering (Figure 5 b). The third fault is a perpendicular cut on the outerring (Figure 5 c) and the fourth fault consists of a cut in a ball (Figure 5 d). Faults (a) and (b) are similar to the faults of the real system.

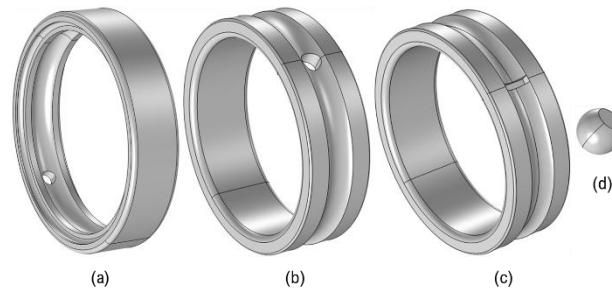


**Figure 5 :** Modelled faults, (a) Inner race fault 1 (b) Outer race fault (c) Inner race fault 2 (d) Ball fault

All bearing components are modelled using DIN 17230 100Cr6 material. The shaft, bearing pedestals and motor housing are modelled using the default COMSOL structural steel material.

Bearing cages are provided with free displacement nodes to prevent restrictions on the rotation axis. Hinge joints are used at each cage socket to permit the relative rotation of the balls in the cages (Figure 6). Clearance between each ball and cage socket is provided, and internal contact is modelled using simplified penalty parameters in the clearance joints. All geometric dimensions of the bearings, as well as other bearing parameters available from the SKF datasheet, are adopted as per the twin bearing track to avoid initial overlapping of geometries. Such as the gap between the bearing balls and the races is 0.09 mm.

The base boundaries are fixed to the ground using fixed elastic joints. Acceleration measurements are recorded from the top plate of the central ball-bearing pedestal, similar to the sensor location of the real system (Figure 4).

## 4.2 Contact Settings

The model utilises the rigid body contact node in COMSOL MBD, which applies the penalty force algorithm to simulate contact forces in non-deformable rigid domains. Here, a



centre-based contact method is used. The gap between the balls and the races is computed at every step. The gap is determined by the distance between the centres and the radii of the two bodies considered to be coming in contact. (Figure 6).

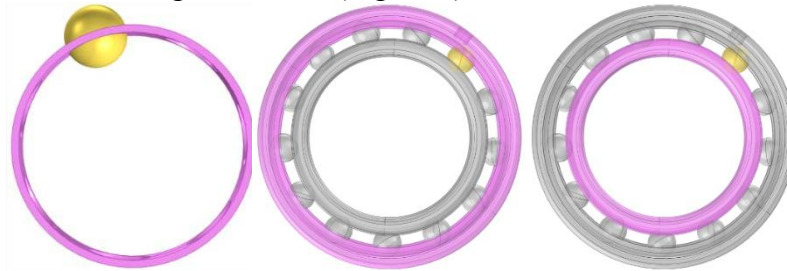


**Figure 6 :** Hinge joint (left), Outer race - Ball contact (middle), Inner race - Ball contact (right)

When modelling the outer race and ball contact, the inside boundaries for contact should only be enabled. Dynamic penalty and automatic penalty factor control are selected for the contact force formulation to have an additional damping coefficient depending on the gap rate. The penalty factor multiplier and the characteristic time are provided during the contact setting. Tangential forces are modelled using the continuous Coulomb friction model. The applied friction model consists of two parts: static and kinetic. The friction attribute can be added to the rigid body contact node to include the tangential forces. Two contact nodes must be created for each ball, defining the inner and outer race contact for all three bearings.

#### 4.3 Meshing and solver

The contact mechanics formulation in COMSOL employs an asymmetric algorithm where contact nodes on the destination surface connect to nodes on the source surface. Contact computations require a finer mesh size to generate accurate stresses, regardless of domain definitions. To achieve optimal meshing, separate nodes are created for different parts of the bearing track, utilising user-controlled meshing. The inner surface boundaries of the outer race, the outer surface boundaries of the inner race that come into contact with the bearing balls, and the balls themselves are primarily considered for meshing optimisation. The mesh of the bearing raceway contact boundaries is twice as fine as that of the rolling balls. The balls are meshed using tetrahedral elements, while only the raceway boundaries that come into contact with the balls are meshed using 2D elements - free triangular nodes. The rest of the bearing and model are meshed with coarser tetrahedral elements adapted for ease of calculation.



The MBD model is evaluated as a time-dependent study using the Backward Differentiation Formula (BDF) scheme for time-stepping by the solver and the PARDISO direct solver. An automatic (Newton) non-linear method is selected for the fully coupled sub-node to handle the non-linearities in the system. The time step of the study is set to  $2.5e-5$  sec. to match the sampling frequency of the experimental measurements. The solver's steps are intermediate, with an automatic maximum step constraint to allow the solver to manage the solution's convergence shifts. Rigid body accelerations in the sensor attachment boundary's x, y, and z directions are defined as global datasets.

## 5 RESULTS

Tests on the bearing track are conducted at 3000 rpm, and both experimental and simulated data are recorded at 40 kHz. The recorded data has 160001 samples, each corresponding to 0.4 seconds of vibration data and is taken from the same location on the Real and Twin bearing track. Therefore, only simulated inner and outer raceway faults are compared for twin model analysis. The Twin models are simulated for 0.4 seconds each and the actual measurement signals are split to match the same number of samples as the simulated signal for signal analysis. Two Twin models are presented for the inner race fault (hole and groove), and one for the outer race fault.

The experimental signal from the real system shows higher energy for outer race fault (RMS 4.3304) than inner race fault (RMS 2.2320), while in the case of twin vibrations, inner race faults have a slightly higher RMS (5.4482) than the outer race fault (RMS 5.2787) (Figure 7). In the second inner raceway fault (groove), the vibration signals (RMS 2.627) are comparable to the actual fault size, due to fault width being closer to the actual fault size. Notably, the amplitudes of the twin signals depend on the penalty factor. The signals from the real system and the Twin models are displayed in Figure 7.

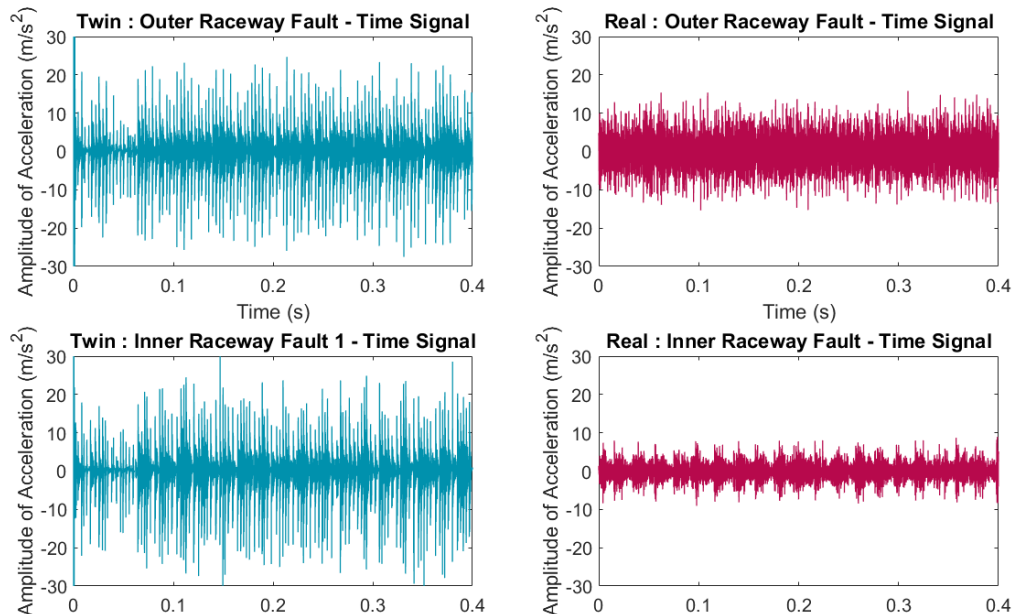
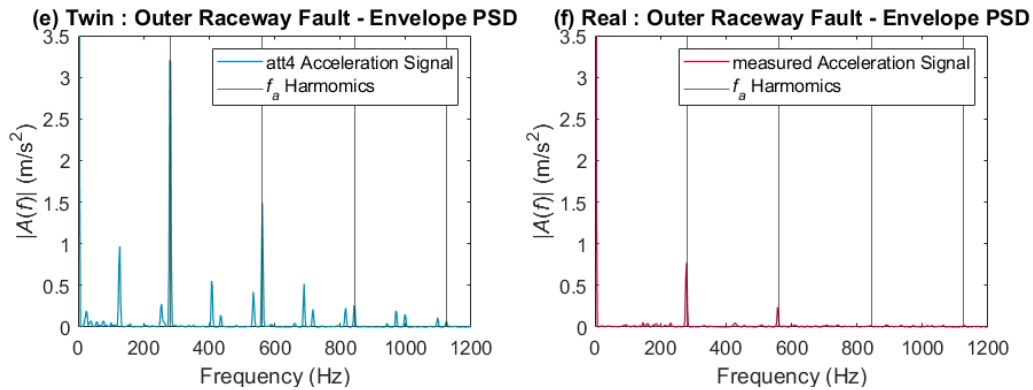


Figure 7: Acceleration time signals

The bearing characteristic fault frequencies are calculated from the bearing geometric parameters: (Rollover frequency outer race fault) = 281.25 Hz, (Rollover frequency inner race fault) = 368.75 Hz. Amplitude peaks at typical fault frequencies of a bearing spectrum are used to ascertain the bearing fault. Vibration frequency amplitudes are extracted using power spectral density (PSD) and envelope analysis. The spectrum correlates to the deviations in the amplitude over various frequencies that are excited depending on the present fault and running machine parameters. When the balls contact the fault boundaries, the response impulse changes as the ball enters and exits the fault. The time interval of the fault is related to the size of the fault. The normal and tangential contact variations might disturb the time interval between the impacts, leading to slippages. These slippages may cause variations in the simulated model's overall amplitude peaks (fault events) resulting from delays in the rotational interval of the balls, affecting the periodicity of the critical frequencies recorded. Therefore, a degree of tolerance is considered for the identification of peaks around critical frequencies. Envelope spectra in the case of the outer and inner raceway faults are shown below. The ball fault could not be identified clearly from the respective Twin's spectrum and hence omitted from the results.



**Figure 8:** Outer raceway fault Frequency spectrum (Envelope PSD)

Envelope spectra are extracted from the real and Twin bearing readings in the case of the outer race fault (Figure 8). The overall trend of the envelope curves of both signals is similar, and the fault frequencies are visible for both systems. After window correction, the peaks of the Twin system have almost three times more amplitude than the real system's. The twin spectrum contains side band frequencies around each harmonic of  $f_a$  and frequencies that can also be found on the real bearing measurements, which are suspected to be present because of low damping in the fixed joint between the outer race and the bearing pedestals.

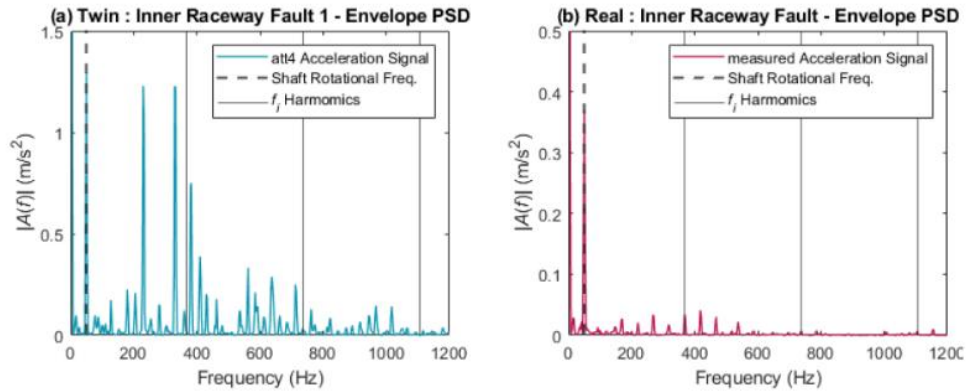


**Figure 9 :** Inner raceway fault 1 Frequency spectrum (Envelope PSD)

The PSD of inner race fault 1 envelope signals are shown in figure 9. The plots clearly show the shaft rotational frequency at 50Hz, which is also the highest peak amplitude for both models. The first harmonic of the inner race damage frequency along with sidebands at shaft frequency is clearly visible for the real system at 368.75 Hz. There are two more harmonics of  $F_i$  present; however, their amplitude is below the relative warning level. In the twin envelope curve, only the second harmonic of the  $F_i$  is visible directly at a resolved amplitude of 0.03 dB/Hz. A peak at 382.5 Hz is present close to the damage harmonic of the inner race.

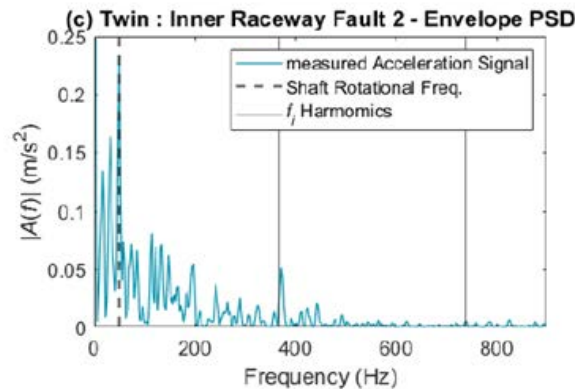


**Figure 10:** Inner raceway fault 2 Frequency spectrum (Envelope PSD)

Figure 10 shows the spectra in the case of the second inner race fault. Multiple harmonics of are visible throughout the spectrum, along with rotational frequency sidebands similar to the real system. The shaft frequency is visible distinctly along with its fourth harmonic at 200Hz, overall, these signals matched better with the real inner race fault.

## 6 CONCLUSION

A model-based DT was built for a rotary machine system that accurately represents various rolling bearing faults. COMSOL Multiphysics was used to simulate complex working conditions matching realistic asset environments, providing insights for adjustments in the overall twin system design and operating process. The twin model can be used to extract

various asset health indicators e.g. RMS and fault frequencies. However, some physics are computationally expensive to resolve compared to others, such as contact settings, which require the most attention. Despite to the expensive computational speed of data using COMSOL v5.6 and the ability to couple multiple physical conditions onto a single model, the application proves to be realistic. The results show that the Twin signals show characteristics of outer and inner race faults with comparable amplitudes, proving the possibility for use in fault diagnosis algorithms. However, the results rely primarily on the shape of the fault and penalty factor, which can be seen in the case of a better similarity between the inner race fault two compared to the real signal. In future studies, the intention is to enhance the Digital Twin for more efficient generation of larger data basis. A thorough description of the Digital Twin's design, encompassing both the bearing and motor track and optimisation processes utilising penalty methods, will be presented in later publications.

## REFERENCES

- [1] Mario Hermann, Tobias Pentek, and Boris Otto, "Design Principles for Industrie 4.0 Scenarios: A Literature Review," 2015.
- [2] Xiaoyang Liu, Haizhou Huang, and Jiawei Xiang, "A Personalised Diagnosis Method to Detect Faults in a Bearing Based on Acceleration Sensors and an FEM Simulation Driving Support Vector Machine," *Sensors (Basel, Switzerland)*, p. 20(2):420, 2020.
- [3] M. Grieves, "Digital Twin: Manufacturing Excellence through Virtual Factory Replication," 2015.
- [4] NEC, "The Future of Digital Twins: NEC Insights".
- [5] S. Erikstad, "Merging Physics, Big Data Analytics and Simulation for the Next-Generation Digital Twins," 2017.
- [6] Azad M. Madni and Michael Sievers, "Model-based systems engineering: Motivation, current status, and research opportunities," *Systems Engineering* 21.3, p. 172–190, 2018.
- [7] G. Ritto, F.A. Rochinha, "Digital twin, physics-based model, and machine learning applied to damage detection in structures," *Mechanical Systems and Signal Processing*, vol. 155, 2021.
- [8] S. Tyagi and S. K. Panigrahi, "Transient Analysis of Ball Bearing Fault Simulation using Finite Element Method," *Journal of The Institution of Engineers (India)*, p. 309–318, 2014.
- [9] Mishra, A. K. Samantaray, and G. Chakraborty, "Ball bearing defect models: A study of simulated and experimental fault signatures," *Journal of Sound and Vibration* 400, pp. 86-112, 2017.
- [10] S. Bazaraa, Hanif D. Sherali, and C. M. Shetty, *Nonlinear programming: Theory and algorithms*, Wiley-Interscience and Chichester : John Wiley, 2006.
- [11] M. Adel and M. M. Khader, "Numerical Simulation Using GEM for the Optimization Problem as a System of FDEs," *Applied Mathematics* 08.12, p. pp.

- 1761–1768, 2017.
- [12] M. Neto, M. C. Oliveira, and L. F. Menezes, "Surface Smoothing Procedures in Computational Contact Mechanics," *Archives of Computational Methods in Engineering* 24.1, p. 37–87, 2017.
  - [13] COMSOL, "Spherical to Spherical Formulation. COMSOL - Software for Multiphysics Simulation".
  - [14] COMSOL, "Theory of Rigid Body Contact. COMSOL - Software for Multiphysics Simulation".
  - [15] Li, Shuting, "A mathematical model and numeric method for contact analysis of rolling bearings. Mechanism and Machine Theory," 2018.
  - [16] COMSOL, "Theory of friction in rigid body contact. COMSOL - Software for Multiphysics Simulation".
  - [17] K. Davey, "Induction Motor Analyses International TEAM Workshop Problem 30".